

Nonequilibrium “Melting” of a Charge Density Wave Insulator via an Ultrafast Laser Pulse

Wen Shen,¹ Yizhi Ge,¹ A. Y. Liu,¹ H. R. Krishnamurthy,^{2,3} T. P. Devereaux,^{4,5} and J. K. Freericks¹

¹*Department of Physics, Georgetown University, Washington, D.C. 20057, USA*

²*Jawaharlal Nehru Centre for Advanced Scientific Research, Bangalore 560012, India*

³*Department of Physics, India Institute of Science, Bangalore 560012, India*

⁴*SLAC National Accelerator Laboratory, Stanford University, Stanford, California 94305, USA*

⁵*Geballe Laboratory for Advanced Materials, Stanford University, Stanford, California 94305, USA*

(Received 21 April 2013; revised manuscript received 17 December 2013; published 2 May 2014)

We employ an exact solution of the simplest model for pump-probe time-resolved photoemission spectroscopy in charge-density-wave systems to show how, in nonequilibrium, the gap in the density of states disappears while the charge density remains modulated, and then the gap reforms after the pulse has passed. This nonequilibrium scenario qualitatively describes the common short-time experimental features in TaS₂ and TbTe₃, indicating a quasiuniversality for nonequilibrium “melting” with qualitative features that can be easily understood within a simple picture.

DOI: 10.1103/PhysRevLett.112.176404

PACS numbers: 71.45.Lr, 71.10.Fd, 78.47.J-, 79.60.-i

The theory of second-order equilibrium phase transitions has a long history and is now well understood [1]. In the case of electronic phase transitions induced by electron-phonon interactions, gaps in the electronic excitation spectrum typically open up simultaneously with the formation of long-range charge-density-wave (CDW) or superconducting order in weak coupling, and precede the formation of these orders in strong coupling. Recent experiments in ultrafast pump-probe spectroscopy that investigated layered CDW materials have revealed a new nonequilibrium paradigm where long-range CDW order persists but, by conventional interpretation, the local electronic excitation spectrum becomes gapless (by creating subgap states) for a transient period of time [2–12]. The similarity of these experiments to each other for quite different materials points towards a quasiuniversal behavior in nonequilibrium, whose main features are captured with a simple exactly solvable model that we present below.

We concentrate on two materials that have been measured experimentally. The quasi-two-dimensional material 1T-TaS₂ orders in a three sublattice star-of-David pattern, and develops an insulating gap that is believed to be due to strong electronic correlations [13–15]. In TbTe₃, the system condenses in unidirectional incommensurate CDW stripes, and the order only partially gaps the Fermi surface, leaving the system with metallic conductivity [6,8,16,17]. In both materials, experiments have clearly shown the transient collapse of the CDW gap in the density of states (DOS) as the system is pumped into a nonequilibrium state by a large-amplitude pulse [4–6,8–10]. At picosecond times after the pump pulse, the DOS, as inferred from the time-resolved photoemission spectroscopy (PES), oscillates due to coupling with the soft phonon that is involved in the CDW transition, before the gap fully reforms at longer times. In TaS₂, a pump-probe core-level x-ray photoemission

spectroscopy experiment [7] further shows that the amplitude of the electronic CDW order parameter (given by the difference of the electronic charge density on the different sublattices of the CDW) is reduced by the pulse, but does not vanish; it eventually settles into a long-time value that is reduced from the original size due to heating of the system and relaxation back to equilibrium. Hence, unlike in equilibrium, experiments show that the electronic CDW order parameter and the gap in the electronic energy spectrum become partially decoupled in the sense that the gap collapses while residual modulated CDW order remains.

This change in character of the many-body state has been named a nonequilibrium melting (or phase transition) of the CDW but it has an inherently different character from the equilibrium phase transitions. For example, the gap is initially fragile to the presence of an electric field while the electronic order parameter is initially robust (due to the frozen in lattice distortion yielding an inhomogeneous potential for the electrons), so the behavior of the system during the transient closing of the gap is different from an equilibrium phase transition.

Electrons interact on time scales on the order of a femtosecond, which motivates the hot-electron model [4,5,18,19], where the electrons rapidly thermalize amongst themselves forming a hot quasithermal gas that equilibrates with the phonons on much longer time scales [12,20]. The most interesting quantum regime is the short-time transient one where properties change most rapidly in time and are not described by such simplifications. In particular, a hot electron model can never lead to a closing of the gap in the DOS for short times when the lattice distortion remains frozen in, and the core-hole PES calculations below definitely suggest the latter.

Before introducing the simplified model for the CDW, we show how the electronic order parameter can survive to

hot electron temperatures with a real materials calculation for TaS₂. In a CDW system pumped by a laser pulse, the lattice distortion is frozen in at short times and cannot relax [12]. Hence, the electrons always see a corrugated potential due to the ordered arrangement of the ion cores [21] and respond to that potential by modulating their charge distribution so that the electronic order parameter does not vanish. We illustrate this in Fig. 1, where we calculate the core-level x-ray photoemission spectroscopy for TaS₂ with the lattice distortion fixed at its $T = 0$ value, but the electrons raised to temperatures up to 4000 K. The core-level splitting is proportional to the CDW order parameter of the conduction electrons, indicating that the order decreases but remains for any finite temperature, as seen in experiment [7]. These results were calculated within density-functional theory using the all-electron, full potential code [22] WIEN2K. The Perdew-Burke-Ernzerhof [23] version of the generalized gradient approximation was used to take into account the electron-electron interaction at the standard level done in density-functional theory (see the Supplemental Material [24]).

An electric field pump is described by the Peierls substitution, which is a time-dependent shift of the momentum. Hence, the set of instantaneous energy eigenvalues is independent of the field and is always gapped. But the nonequilibrium DOS is also influenced by how the eigenfunctions change as a function of time, and often has the gap region modified. We examine the simplest model of a CDW insulator, where the ordering is driven by a periodic potential that is equal to zero on the B sublattice and equal to U on the A sublattice of a bipartite lattice with equal numbers of A and B sites (the electrons are at half filling to form an insulator) (see the Supplemental Material [24]). The Hamiltonian, using standard notation for the creation and annihilation operators, is

$$\mathcal{H}(t) = -\sum_{ij} \tau_{ij}(t) c_i^\dagger c_j + (U - \mu) \sum_{i \in A} c_i^\dagger c_i - \mu \sum_{i \in B} c_i^\dagger c_i \quad (1)$$

with the chemical potential satisfying $\mu = U/2$ for half filling and the time-dependent hopping given by the Peierls substitution (see the Supplemental Material [24]) in the presence of the pump pulse. The fixed underlying potential in our model mimics the lattice distortion, which does not change for short transient times. In equilibrium, the DOS develops a gap of magnitude equal to U (we choose $U = 1t^*$ throughout here with t^* the renormalized hopping for a hypercubic lattice in infinite dimensions and the initial temperature before the pulse equal to zero). The DOS is reflection symmetric about zero energy on the A and the B sublattices [see Fig. 2(a)]. On one lattice, there is a pileup of states, which gives a divergence that grows like the inverse square root at the lower gap edge, while on the other, the singularity lies at the upper gap edge (these singularities govern much of the behavior and are

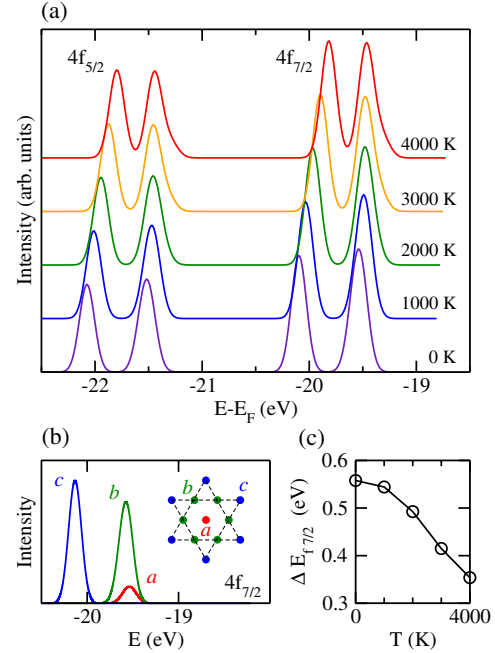


FIG. 1 (color online). Calculated Ta $4f$ core-level photoemission spectrum for the commensurate CDW phase of 1T-TaS₂. (a) Dependence of the spectrum on electronic temperature in the hot electron model. The $f_{5/2}$ and $f_{7/2}$ levels are split due to spin-orbit coupling (2 eV) and further split due to the existence of three inequivalent Ta sites in the CDW phase (0.5 eV). (b) Site-projected contributions to the $f_{7/2}$ spectrum. The $4f$ levels on Ta a and b sites lie close in energy and combine into a single peak. Inset is the star-of-David structure for the CDW (a red, b green, and c blue). (c) Electronic-temperature dependence of the splitting between the $a - b$ and c peaks in the $4f_{7/2}$ spectrum.

independent of dimension). The Fourier transform of such a DOS can be shown to oscillate with an amplitude that decays with an inverse square root of time.

We model the laser pulse by a one and a half cycle electric field that approximately runs from a time of $-15h/t^*$ to $15h/t^*$ with an amplitude E_0 at $t = 0$ that can be adjusted and is shown in Fig. 4(d). The exact solution of this nonequilibrium CDW (including a solution for the pump-probe PES signal [25]) requires one to use a Kadanoff-Baym-Keldysh formalism [26–28]. We solve for the retarded and lesser Green's functions, which depend on two times [26] (t and t') using an exact evolution operator that can be expressed as a direct product of 2×2 matrices for each momentum point in the small Brillouin zone, and evaluated via the Trotter formula (see the Supplemental Material [24]). The solution is complicated because the different terms in the Trotter formula do not commute.

We redefine the Green's functions in terms of the Wigner coordinates corresponding to the average [$t_{\text{ave}} = (t + t')/2$] and relative [$t_{\text{rel}} = t - t'$] times. The transient DOS at t_{ave} is then defined to be the imaginary part of the Fourier transform of the retarded Green's function with respect to t_{rel} . Similarly, the time-resolved PES response

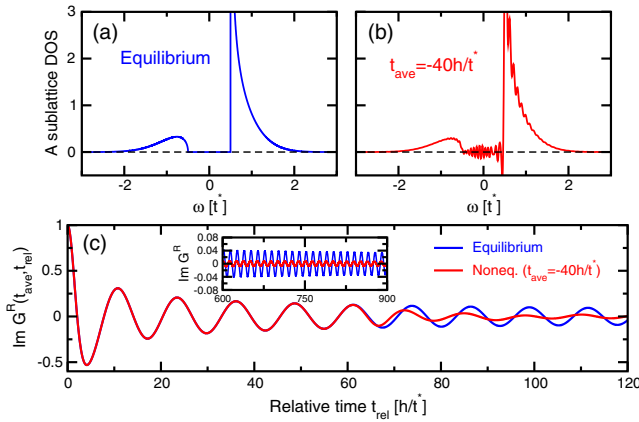


FIG. 2 (color online). (a) The equilibrium local DOS on the A sublattice. (b) The nonequilibrium local DOS for $E_0 = 0.75$ at an average time $-40h/t^*$. (c) Imaginary part of the retarded Green's function in real time. The inset shows that the retarded Green's function has a long temporal tail.

function is found from a probe-pulse-weighted Fourier transform of the lesser Green's function [19,25]. The Green's functions are nonlocal in time and they have long tails as functions of relative time; hence, the pump pulse can modify them both at the time of the pulse, and for long average times before or after the pulse has ended.

We illustrate this with the DOS in Fig. 2, which shows how the gap region can be significantly changed even for average times far before the pulse is turned on. Note that because this is a nonequilibrium situation, the DOS can become negative (due to no Lehmann representation for transient times), implying that the standard interpretation of the DOS fails for transient times. For example, even at a time $40h/t^*$ before the center of the pulse acts on the system ($25h/t^*$ before the pulse starts), we can see that the gap region of the DOS is significantly changed [Fig. 2(b)]. One can directly trace this to the change of the Green's function starting at a relative time of about $60h/t^*$ and continuing to long times ($t_{\text{rel}}^{\text{max}} \approx 10^6 h/t^*$). The Green's function “feels” the effect of the field, because one time is before and one after the field has been turned on, leading to the fragile gap in the DOS.

We show the time-resolved PES signal for an electric pulse amplitude satisfying $E_0 = 0.75$ in Fig. 3, using a probe pulse that has a Gaussian envelope with a width of $14h/t^*$ (the “gap” in the time-resolved PES signal is more robust than in the DOS due to the finite width of the probe pulse, which limits the range in time for the Fourier transform, bypassing some effects due to the long tails, and the fact that the PES signal is always manifestly non-negative). One can see that in the range of average time from about $-20h/t^*$ up to about $20h/t^*$ the gap disappears, and then reforms for longer times. We also see a significant transfer of electrons from the lower to the upper band due to the nonequilibrium pumping of energy into the system. The

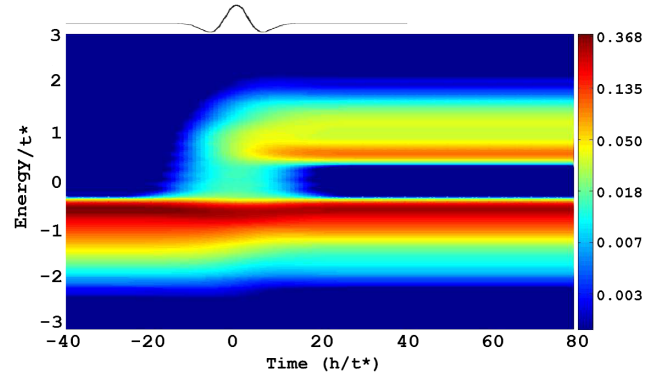


FIG. 3 (color online). Calculated time-resolved PES at $T = 0$ with $E_0 = 0.75$ and averaged over the A and B sublattices, plotted in false color. The electric field is shown above the plot. Movies of this time evolution can be found with the Supplemental Material for $E_0 = 0.75, 1.0,$ and 1.25 [24].

system does tend toward a steady state at long times, but it is not thermal because there is no electron scattering to thermalize the excited electrons. These results are similar for $E_0 = 1$ and $E_0 = 1.25$ (see the Supplemental Material [24]).

Figures 4 and 5 provide summaries of the various features of the nonequilibrium “phase transition.” Figure 4(a) shows the PES signal at $\omega = 0$ as a function of time for a range of different probe pulse widths (full width at half maximum) at a pulse amplitude $E_0 = 0.75$. One can clearly see that the suppression of the gap (by filling in subgap states) is robust once the width is large enough. The inset shows how the gap magnitude grows with the field amplitude, but the width in time remains the same. Figure 4(b) shows that the electronic CDW order parameter of the conduction electrons is reduced due to the pump pulse but does not vanish at $E_0 = 0.75$. For $E_0 = 1$, the order parameter barely touches zero for an instant and then recovers to a small positive value. For $E_0 = 1.25$ and 1.5 , a small reversal of the order is found in this system, which remains reversed after the electric field pulse has gone. The steady state arises because this system is a closed system and the only exchange of energy occurs when the electric field pulse is present. All of these order parameters have oscillations with a period of $2\pi/U$ at long times, which eventually are dephased, as does the current in Fig. 4(c) (the definition is given in the Supplemental Material [24]).

In Fig. 5, we see complex behavior for the expectation value of the total energy $\mathcal{E}(t) = \langle \mathcal{H}(t) \rangle$ while the pulse is on ($E_0 = 0.75$), eventually settling down to a constant value. We can use this steady-state energy to estimate the effective temperature of the system, by calculating the energy as a function of temperature for the system in equilibrium, and setting the temperature by equating to the nonequilibrium energy after the pulse (yields $k_B T = 2.38t^*$). We also can calculate the filling in the

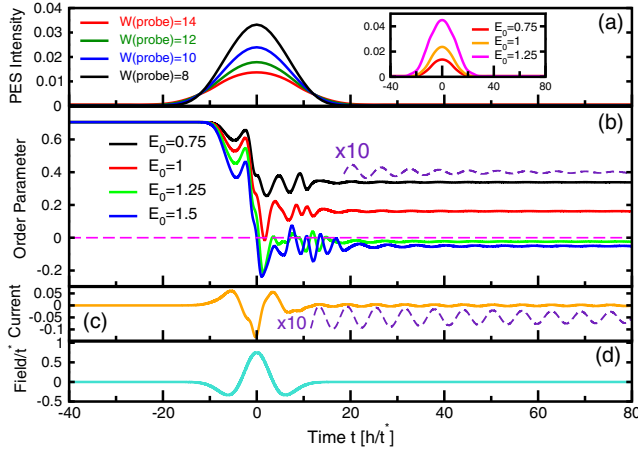


FIG. 4 (color online). (a) Calculated time-resolved PES signal at the Fermi energy with different probe pulse widths and $E_0 = 0.75$. Inset: the same result for the widest width probe pulse but different E_0 values. (b) Conduction electron order parameter for the CDW as a function of time for different pulse amplitudes (zero is indicated by the magenta dashed line). (c) Transient current for $E_0 = 0.75$. With a small field, the current follows in phase with the electric field. For time delays after the pump pulse, the oscillations in the current have the same frequency as the order parameter has ($2\pi/U$, enhanced purple dashed line). (d) Pump pulse electric field with amplitude $E_0 = 0.75$.

lower and the upper bands of the CDW as a function of time for the nonequilibrium case [Fig. 5(b)], and compare it to the equilibrium fillings in each band as a function of temperature. This yields $k_B T = 1.67t^*$ (for $E_0 = 1$ the energy temperature is $3.91t^*$ and the filling one is $3.33t^*$ while for $E_0 = 1.25$ the energy temperature is $31.5t^*$ and the filling one is a negative temperature $-2250t^*$). In thermal equilibrium, these two temperatures must agree. Their difference is one measure of the nonthermal nature of the final state. What is remarkable is that this noninteracting system can remain fairly close to a thermal distribution for small amplitudes of the field. The energy approaches a constant before the current does, because no energy can be added to the system when the electric field vanishes since $d\langle\mathcal{H}(t)\rangle/dt = -\mathbf{E}(t) \cdot \langle\mathbf{j}(t)\rangle$.

Conclusion.—In this work we have shown that a new paradigm exists in nonequilibrium, where driving a CDW system with large fields can cause the gap to transiently vanish for intermediate times in the presence of a generically reduced order parameter. We find this behavior with an exact solution of a simplified model of a CDW insulator described by a staggered potential that is different on one of two sublattices. While this exact solution does not capture all of the quantitative details of the experiments (particularly when coupling of electrons to phonons becomes important), for short and intermediate times it provides a consistent qualitative explanation of the experimental data and is consistent with the emergence of a quasiuniversal

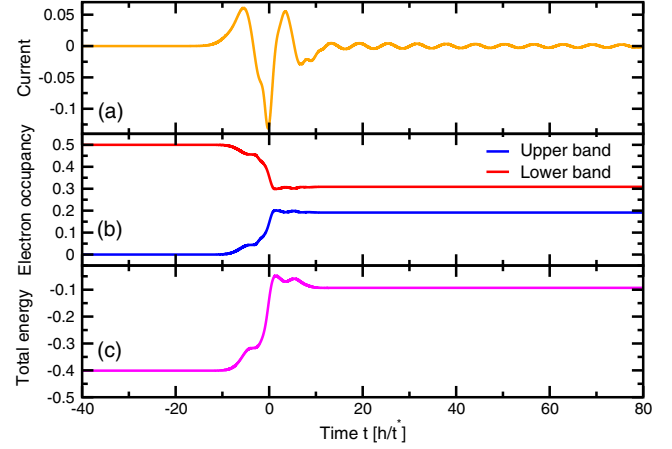


FIG. 5 (color online). Calculated current (a), transient filling of the upper (red) and lower (blue) bands (b), and total energy (c) for the CDW system with $U = 1$ and $E_0 = 0.75$.

behavior in nonequilibrium. The time scale for the reopening of the gap is smaller in this model than in experiment because we have not included a phonon bath that couples to the electrons via the electron-phonon coupling. This allows for an oscillating transfer of energy back and forth between electrons and phonons, until they are damped. When the phonons transfer energy back to the electrons, it is similar to repumping the electrons by an external pulse, which we believe is why the gap remains closed for a longer time in experiments.

The calculations of the core-level x-ray PES in the hot electron model was supported by the National Science Foundation under Grant No. DMR-1006605. The development of the parallel computer algorithms for the time-resolved PES calculations was supported by the National Science Foundation under Grant No. OCI-0904597. The data analysis and application to experiment was supported by the Department of Energy, Office of Basic Energy Research under Grants No. DE-FG02-08ER46542 (Georgetown), No. DE-AC02-76SF00515 (Stanford and SLAC), and No. DE-SC0007091 (for the collaboration). High performance computer resources utilized the National Energy Research Scientific Computing Center supported by the Department of Energy, Office of Science, under Contract No. DE-AC02-05CH11231. J. K. F. was also supported by the McDevitt bequest at Georgetown. H. R. K. acknowledges support from DST (India). The Indo-US collaboration was supported by the Indo-US Science and Technology Forum under a center grant numbered JC-18-2009.

[1] P. M. Chaikin and T. C. Lubensky, *Principles of Condensed Matter Physics* (Cambridge University Press, Cambridge, England, 1995).

- [2] J. Demsar, L. Forró, H. Berger, and D. Mihailovic, *Phys. Rev. B* **66**, 041101(R) (2002).
- [3] V. Brouet, W. L. Yang, X. J. Zhou, Z. Hussain, N. Ru, K. Y. Shin, I. R. Fisher, and Z. X. Shen, *Phys. Rev. Lett.* **93**, 126405 (2004).
- [4] L. Perfetti, P. A. Loukakos, M. Lisowski, U. Bovensiepen, H. Berger, S. Biermann, P. S. Cornaglia, A. Georges, and M. Wolf, *Phys. Rev. Lett.* **97** 067402 (2006).
- [5] L. Perfetti, P. A. Loukakos, M. Lisowski, U. Bovensiepen, M. Wolf, H. Berger, S. Biermann, and A. Georges, *New J. Phys.* **10**, 053019 (2008).
- [6] F. Schmitt *et al.*, *Science* **321**, 1649 (2008).
- [7] S. Hellmann *et al.*, *Phys. Rev. Lett.* **105**, 187401 (2010).
- [8] F. Schmitt, P. S. Kirchmann, U. Bovensiepen, R. G. Moore, J.-H. Chu, D. H. Lu, L. Rettig, M. Wolf, I. R. Fisher, and Z.-X. Shen, *New J. Phys.* **13**, 063022 (2011).
- [9] J. C. Petersen *et al.*, *Phys. Rev. Lett.* **107**, 177402 (2011).
- [10] N. Dean, J. C. Petersen, D. Fausti, R. I. Tobey, S. Kaiser, L. V. Gasparov, H. Berger, and A. Cavalleri, *Phys. Rev. Lett.* **106**, 016401 (2011).
- [11] T. Rohwer *et al.*, *Nature (London)* **471**, 490 (2011).
- [12] M. Eichberger, H. Schäfer, M. Krumova, M. Beyer, J. Demsar, H. Berger, G. Moriena, G. Sciaini, and R. J. D. Miller, *Nature (London)* **468**, 799 (2010).
- [13] P. Fazekas, in *Modern Trends in the Theory of Condensed Matter*, Lecture Notes in Physics, edited by A. Pekalski and J. A. Przystawa Vol. 115 (1980) p. 328.
- [14] X. Wu and C. Lieber, *Science* **243**, 1703 (1989).
- [15] J.-J. Kim, W. Yamaguchi, T. Hasegawa, and K. Kitazawa, *Phys. Rev. Lett.* **73**, 2103 (1994).
- [16] A. Fang, N. Ru, I. R. Fisher, and A. Kapitulnik, *Phys. Rev. Lett.* **99**, 046401 (2007).
- [17] V. Brouet *et al.*, *Phys. Rev. B* **77**, 235104 (2008).
- [18] P. B. Allen, *Phys. Rev. Lett.* **59**, 1460 (1987).
- [19] J. K. Freericks, H. Krishnamurthy, Yizhi Ge, A. Y. Liu, and Th. Pruschke, *Phys. Status Solidi B* **246**, 948 (2009).
- [20] T. Hertel, E. Knoesel, M. Wolf, and G. Ertl, *Phys. Rev. Lett.* **76**, 535 (1996).
- [21] M. D. Johannes and I. I. Mazin, *Phys. Rev. B* **77**, 165135 (2008).
- [22] K. Schwarz and P. Blaha, *Comput. Mater. Sci.* **28**, 259 (2003).
- [23] J. P. Perdew, K. Burke, and M. Ernzerhof, *Phys. Rev. Lett.* **77**, 3865 (1996).
- [24] See Supplemental Material at <http://link.aps.org/supplemental/10.1103/PhysRevLett.112.176404> for technical descriptions of the calculations and formalism and for movies that animate cross-sectional cuts through Fig. 3.
- [25] J. K. Freericks, H. R. Krishnamurthy, and Th. Pruschke, *Phys. Rev. Lett.* **102**, 136401 (2009).
- [26] L. P. Kadanoff and G. Baym, *Quantum Statistical Mechanics* (Benjamin, New York, 1962).
- [27] L. V. Keldysh, *Zh. Eksp. Teor. Fiz.* **47**, 1515 (1964) [*Sov. Phys. JETP* **20**, 1018 (1965)].
- [28] G. D. Mahan, *Many-Particle Physics* (Springer-Verlag, Berlin, 2000), 3rd ed.